# Simulation of Everting Tube Experiments

Blake Hannaford

July 19, 2024

# 1 Introduction

## 1.1 Literature Review

Prior studies of eversion mechanics have relied on the assumption of constant pressure over time and throughout the extent of the device. Blumenschein et al.[1] applied biomechanical models for plant shoot growth to analogous physical processes in everting tubes and compared simulations with experimental measurements. Notably, for the speeds and design parameters they studied, they did not find an effect indicating air flow resistance between the housing and the everting tube. [**?**] Performed mostly quasi-static modeling of ETs but studied the important buckling phenomena in complex geometric environments which we do not consider here.

[2] created a dynamic, lumped parameter mechanical model of eversion with special emphasis on friction properties between an everting tube and its environment as well as a second contact between the tube and a rod (catheter) in contact with the everted material. This work is close in spirit to ours, but their eversion system was controlled by an "active channel" to which the inner part of the everting tube was connected. Thus eversion was only possible as allowed by active channel motion. This work studied slower rates of eversion (0-6$mmsec^{-1}$) and did not compare time responses, instead comparing velocity which was apparently constant under measured conditions. They measured a "breakway" pressure of 115kPa which was comparable to our experiments. This model included a sophisticated friction model having static, Coulomb, and viscous components.

## 1.2 Observed Eversion Characteristics

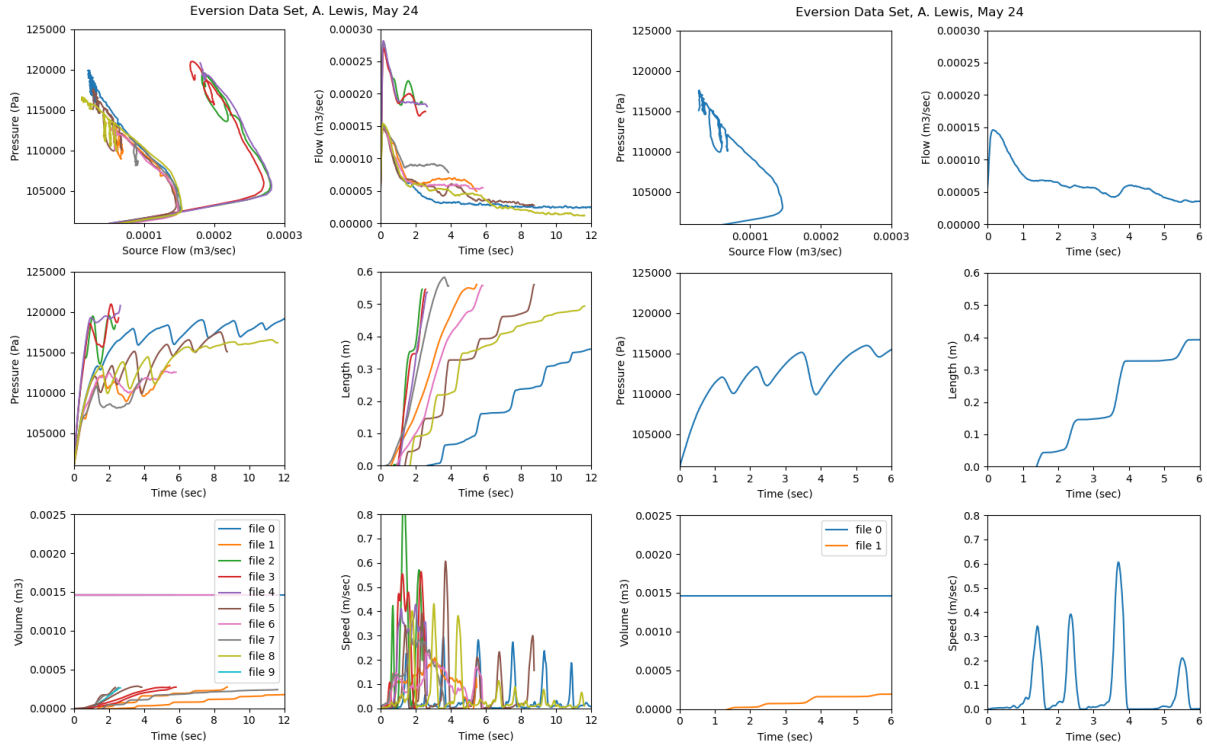


Figure 1: Experimental data displaying dynamic characteristics of loaded eversion. All data (Left), single example (Right) note different time axes for the two plots. (See Lewis, Fig 9. Loads: high inertia, high Friction)

****** Resolve 10x flow rate hack!!! *****

Recently, Lewis [**?**] measured some complex dynamic behaviors of a tube everting inside a straight support tube of approximately the same diameter (25mm) as the inflated tubing material (Figure 1, Left panel). Data consist of 9 trials on 3 tubes. Tube #1 had 4 trials, tube #2 had 2 trials, and tube #3 had 3 trials. Tubes were supplied by a reel which was free to rotate inside the pressure vessel (housing). Variable loads could be applied to the reel including inertia and coulomb friction. Applied loads are given in Table **??**.

There are two distinct clusters of responses, five slower and three faster (particularly clear in the flow plots (top row). The three datasets having higher flow rates in the top row of Figure 1 are the three trials of tube #3.

One experiment which displays several interesting evertion characteristics is shown in Figure 1, Right Panel. Referring first to the length-vs-time plot (middle right), we see a start-stop or staircase behavior sometimes seen with eversion under relatively constant input pressure. It should be noted that the selected eversion experiment (Right panel) was loaded by "high" inertia and "High" friction applied to the reel. Velocity (lower right) indicates a series of peaks where the eversion "breaks-free" but then stops again a short time later giving length-vs-time a stair-step characteristic.

Pressure (middle left) first grows for about 1 second without corresponding eversion motion, and then oscillates in approximate synchrony with the velocity peaks.

Finally, the pressure-flow phase plot (top left) shows a predominantly diagonal straight line slope. Flow grows rapidly and then the trajectory proceeds from lower right (high initial flow with low pressure) to upper left (lower flow, higher pressure). The trajectory makes loops to lower pressures and back up to the slope at higher pressures. These loops correspond in time to the pressure oscillations (middle left).

These dynamic characteristics (start-stop bursting, pressure oscillations, diagonal phase trajectory, and downward loops) were not all present under all experimental conditions. In summary then, depending on factors to be determined, some or all of these characteristics may or may not be present in a given free eversion run.

## 1.3 Simulation Goals

The goals of this simulation are:

1. Increase fundamental understanding of the eversion process.
2. Identify key parameters capable of representing the complex dynamic characteristics above.
3. Identify values and value ranges for unknown parameters which fit individual experiments.
4. Clearly segregate the parameters into known, measured quantities vs. free parameters.
5. Codify an efficient manual method for parameter identification.

In any simulation study caution must be exercised when there are a large number of free parameters as there may be several combinations of parameters or manifolds in the parameter space which may fit any dataset. In Section 2.2, below, we review the overall parameter set and classify the parameters into known, independently measureable parameters vs free parameters.

## 1.4 Dynamic Model

The dynamic model of an eversion drive system includes;

- An everting tube of length $L$ and growth rate $\dot{L}$.
- A pressurized housing
- A reel with rotation $\theta, \dot{\theta}, \ddot{\theta}$, on which tubing is rolled having inertia (assume fixed) of $J$ and radius $r$.
- A brake which applies a Coulomb friction torque to the reel

$$\tau_c = C\text{sgn}(\dot{\theta})$$

- A "crumple zone" in which eversion material can accumulate between the reel and the everting tube. The length of material in the crumple zone is $L_c >= 0$.

- Eversion happens when the eversion force (pressure × face area of the tube) exceeds any retarding forces.
- Forces which can oppose eversion include,
  - drag forces and inertial forces required to pull the tubing material inside the deployed tube,
  - reel inertia and reel friction resulting from unspooling material (only when $L_c = 0$).

The everting tube can be in one of two states:

- GROWING (the tube is actively everting, $\dot{L} > 0$)
- STUCK (the tube is not growing due to insufficient everting force, $\dot{L} = 0$)

and the reel/crumple zone can be in one of two additional states:

- TAUGHT (the crumple zone has zero length , $L_c = 0$)
- SLACK (there is material in the crumple zone, $L_c > 0$)

Together the system can be in four states comprising the permutations of these two state variables.

# 2 Model Structure and System Equations:

We will consider two possible structures:

A *one-compartment* model (Figure 2, Left) assumes that first-order pressure dynamics are present between a source of pressure ($P_{source}$ from a compressor, regulator, or tank accumulator) and a single everting tube system volume (housing plus tube volume, $V_{et} = L \times \pi r^2$.) with uniform pressure, $P$.

The *two-compartment* model(Figure 2, Right) assumes that additional first-order pressure dynamics are present between the housing volume (pressure, $P_1$, volume $V_{housing}$ and the tube system volume ($V_{et}$ as above).

For both structures, we can make the tube radius a function of its length, $R_{et}(L)$. This can simulate novel designs with varying radii exploiting new ET fabrication methods such as laser welding or CNC heat sealing.

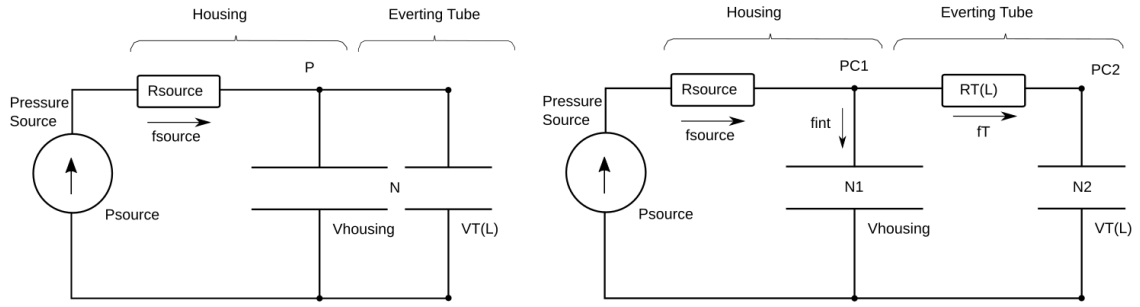


Figure 2: Two model structures applied to eversion experiments of Fig. 1 expressed as simple electric circuits. One compartment model (Left) lumps the housing volume and tube volume together. Two compartment model (Right) introduces length-dependent resistance between the housing and tube, $RT(L)$, to split the pressure state, $P$ into two states, $P_{C1}, P_{C2}$.

After setting initial conditions (see below), we model eversion dynamics by:

1. Computing volume and pressure.
2. Computing forces applied to the eversion tip and accounting for the mechanical advantage (everting material speed is $2 \times \dot{L}$, Pressure applied to everting front develops 1/2 the everting force expected from $P \times A$.)
3. Selecting the dynamic mode from the four combined states above and computing accelerations. GROWING or STUCK state is selected by pressure thresholds (related to net eversion force by $F = PA(L)$. TAUGHT or SLACK state is selected by checking length of the crumple zone material. Then, according to the dynamic mode, summing forces, equating to zero, solving for tube and reel accelerations.

4. Eversion does not come to an instant halt. We empirically model a short exponential decay of velocity as tube decelerates.
5. Implement the transitions between states STUCK, Growing, and TAUGHT, SLACK.
6. Integrate acceleration and velocity to update state variables.

Specifically for the one-compartment model:

1. $$V_t = V_{housing} - V_{contents} + LA \tag{1}$$

   $V_t$ includes both the reel housing volume (minus the volume of its contents) and the everted tube volume $Vet(L)$ with cross sectional area $A(L)$ where

   $$A(L) = \pi Ret(L)^2 \tag{2}$$

   where $Ret(L)$ is initially a constant radius, but can also be a function describing a diameter profile manufactured into the everting tube. Alternatively, $Ret(L)$ can describe a constraining tube of radius $R_C(L)$ such that

   $$R_C(L) <= Ret(L) \tag{3}$$

   When the radius is not constant, tube volume is computed by

   $$Vet = \pi \int_0^L Ret(L)^2 dL \tag{4}$$

   From the ideal gas equation:

   $$P = \frac{NRT}{V_t} \tag{5}$$

   where $N$ is the molar mass of gas in the system, $R$ is the gas constant, and $T$ is the temperature in °K. We assume temperature is constant during eversion (isothermal boundary condition).

2. Computing Forces:

   $$F_{ever} = \max(0, PA/2) \tag{6}$$

   $$F_c = \tau_{Coulomb}/r \tag{7}$$

   Coulomb friction is independent of velocity so does not get scaled by the 2× mechanical advantage.

3. Computing acceleration according to the four dynamic states:
   GROWING and SLACK:

   $$\ddot{L} = \frac{F_{ever} - F_D(FL, \dot{L}) - F_C}{M_T/2} \tag{8}$$

   $$\ddot{\theta} = -\tau_{Coulomb}/J \tag{9}$$

   where $M_T$ is the mass of inside tubing, pulled at 1/2 speed by the eversion process, and $J$ is the rotational inertia of the tubing reel inside the housing. We assume $J$ is constant (despite some material being unspooled) and that $\tau_{Coulomb}$ is a known constant torque. Finally tubing mass is proportional to length: $M_T = L \cdot \text{ET\_mass\_per\_mm}$.

   GROWING and TAUGHT:

   $$\ddot{L} = (F_{ever} - F_D - F_C)/(M_T/2 + J/r^2) \tag{10}$$

   $$\ddot{\theta} = \ddot{L}/r \tag{11}$$

   in this state reel acceleration is kinematically linked to tube growth.

STUCK and (SLACK or TAUGHT):

$$\ddot{L} = -1 * \text{dmax}(0, \alpha * \dot{L}) \tag{12}$$

$$\ddot{\theta} = -\tau_{Coulomb}/J \tag{13}$$

where $\alpha$ is an empirical time constant modeling the dynamics of eversion stopping.

Modeling flow from the pressure source (Thevenin equivalent):

$$Fl_{source} = \frac{P_{source} - P}{R_{source}} \tag{14}$$

Converting airflow ($m^3/sec$) to rate of molar mass flow:

$$\dot{N} = Fl_{source} \cdot \text{moles\_per\_m3} \tag{15}$$

Model velocity and length dependent eversion force which is resistance to pulling out eversion material:

$$F_D(L, \dot{L}) = \max\left(2(K_D + LK_{2D})\dot{L}, F_{end}(L)\right) \tag{16}$$

Where the factor of two accounts for everting material going at twice tube growth rate, $\dot{L}$, and $F_{end}$ is a function to model the everting tube material running into its hard stop:

$$F_{end}(L) = (L/Lmax)^7 P_{source} \pi Ret(L)^2 \tag{17}$$

Update length of crumpled material (if any)

$$L_C = \max(0, r\theta - L) \tag{18}$$

4. Implement state transitions

   We have a switching model to replicate observed intermittent starting and stopping of eversion which updates the state based on current pressure:

$$\texttt{state} = \begin{cases} \text{GROWING}, & P > P2 \\ \text{unchanged}, & P1 <= P <= P2 \\ \text{STUCK}, & P < P1 \end{cases} \tag{19}$$

   We update the crumple state depending on the length of the crumple zone ($L_C$) as

$$\texttt{state2} = \begin{cases} \text{TAUGHT}, & L_C <= 0 \\ \text{SLACK}, & L_C > 0 \end{cases} \tag{20}$$

5. Integrate state variables.

   Finally, we integrate the state variables:

$$\begin{aligned} \dot{L} &= \dot{L} + \ddot{L}dt \\ L &= L + \dot{L}dt \\ \dot{\theta} &= \dot{\theta} + \ddot{\theta}dt \\ \theta &= \theta + \dot{\theta}dt \\ N &= N + \dot{N}dt \end{aligned} \tag{21}$$

   and, if necessary ($Ret(L)$ is not constant),

$$Vet = Vet + \pi Ret(L)^2 \dot{(L)} \tag{22}$$

| Parameter | Class | Value | Units | Description | source |
|---|---|---|---|---|---|
| ET_radius | Known | 12.5 | $mm$ | Tube radius | tube design |
| J | Known | [ 4.67, 5.1, 5.64]$\times 10^{-4}$ | $kg/m^2$ | Reel inertia [Lo, Med, Hi] | design, tests [**?**] |
| Tau_coulomb | Known | [ 2.9, 17.4, 69.4]$\times 10^{-3}$ | $Nm$ | Coulomb friction torque on reel [Lo, Med, Hi] | design, tests [**?**] |
| Lmax | Known | 0.5-0.8 | $m$ | Tube length | tube design |
| Patmosphere | Known | 101.325 | $kPa$ | Atmospheric pressure | |
| RT | Known | 2.5E+3 | $m^3Pa/mol$ | Gas constant x temperature | Ref. |
| T | Known | 2.95E+2 | $^\circ K$ | Room temperature | Thermometer |
| Vhousing_m3 | Known | 1.256E-3 | $m^3$ | Housing air volume | CAD model |
| et_MPM | Known | 0.1 | $kg$ | Tubing mass per meter | measured |
| rReel | Known | | $m$ | Reel radius | CAD model |
| ET_Res_ratio | Free | 0.3—0.6 | dimensionless | ET resistance scale | manual tuning |
| K2drag | Free | 0.16—4.0 | $Nm$ | Empirical Fit | manual tuning |
| Kdrag | Free | 0.15—6.0 | $N/m^2/sec$ | Empirical Fit | manual tuning |
| PBA_static | Free | 107—118.5 | $kPa$ | Break-away pressure | manual tuning |
| PHalt_dyn | Free | 61—116 | $kPa$ | Eversion stopping pressure | manual tuning |
| Psource_SIu | Free | 118—145 | $kPa$ | Gas source pressure | manual tuning |
| Rsource_SIu | Free | (8—14)$\times 10^7$ | $Pa/m^3/sec$ | Slope of P-Fl load-line | manual tuning |
| Thresh. Taper | Free | 640—3800 | $Pa/m$ | Change in thresholds w/ length | manual tuning |

Table 1: Parameters used and their sources and values.

### 2.1 Initial Conditions

For a typical simulation, the initial conditions are

$$\begin{aligned} P &= 1 \text{ atmosphere} \\ \texttt{state1} &= STUCK \\ \texttt{state2} &= TAUGHT \\ N &= N(V_{housing} - V_{contents})/RT \\ L &= 0 \\ \dot{L} &= 0 \\ \ddot{L} &= 0 \end{aligned} \tag{23}$$

### 2.2 Parameters

The model parameters are classified in Table 1. The first 10 parameters are independently measured or otherwise known. For example, atmospheric pressure (Patmosphere) and room temperature (T) are known or measured constants. Reel parameters rReel, J, Tau_coulomb, and Vhousing_m3 are known from CAD files and independently confirmed by measurements[**?**]. Inertia, J, and coulomb friction were set to three different levels during experimentation, "low", "medium," and "high" as indicated in Table 1. The maximum tubing length, Lmax, is known at fabrication time (about 0.6m). Sometimes it was modified within a narrow range by matching the end length between experiment and simulations.

## 3 Parameter Estimation from Data

We used the following process to fit parameters to an eversion data record where the record consists of the following data as a function of time:

- Pressure in the tube storage chamber ($Pa$)

- Air flow from source into tube storage chamber ($m^3/sec$)
- Length of the everted tube ($m$)
- Velocity of eversion (derived) ($m/sec$)

Simuation outputs can be plotted over the data to facilitate comparison.

We can then use the following procedure to iteratively tune the free model parameters to match a particular experimental run.

1. Adjust load line pressure intercept.

   **Data Focus:** Pressure/Flow curves (upper left):
   **Procedure:** Adjust Psource_SIu to move the load line and sim trajectory (they should overlap) up and down. Adjust Rsource_SIu to adjust its slope (higher values slope down more).

2. Adjust stop-start thresholds.

   **Data Focus:** Pressure-Time curves (middle left):
   **Procedure:** Adjust PBA_static up or down to match the pressure peaks in experiment (green dashed). Adjust PHalt_dyn up or down to match the pressure valleys.

3. Adjust threshold taper.

   **Data Focus:** Pressure-Time curves (middle left):
   **Procedure:** Adjust Threshold Taper up or down to speed or slow down convergence of the thresholds.

4. Adjust Friction or drag

   **Data Focus:** Length-Time curves (middle right):
   **Procedure:** Adjust the viscus drag constant of tubing (K_drag) up or down to match the overall slope of the data trace. Adjust max tubing length (Lmax) to match stopping point of data.

5. Experiment with other parameters or go back and repeat the procedure.

We modeled one experiment (hi inertia, hi friction, tube-2, trial-2) simulating the model with an initial set of parameters (Table 2).

A number of features in the experimental data are absent from the simulation output including: load line between pressure and flow are misaligned by an offset and a slight slope difference (Figure 3, upper left), Pressure changes smoothly over time in the simulation without oscillations evident in the experimental data (middle left), and tube length grows smoothly in the simulation compared with discontinuous growth in the data (middle right, lower right).

Using the above procedure, we made the following changes to improve match between simulation and experiment:

1. Reduce source pressure to match the load line to the predominant Pressure-Flow slope.
2. Adjust pressure thresholds for "Break-Away" and "Halting" and drag coefficients to match the bursty motion of the experimental data.
3. Adjust source pressure, drag parameters, and threshold taper to increase matching.

After modifications to some parameters (Table 4), the simulation shows better match to the pressure-flow load line, pressure oscillations during growth, and bursty length changes during growth.

Some remaining differences include: slower rate of change of pressure with time after the initial pressure rise (during eversion) and lack of looping cycles visible in the upper left of the pressure-flow plot. Indeed from the one-compartment model structure (Figure **??**) it is clear that the simulation is constrained to the diagonal load line.

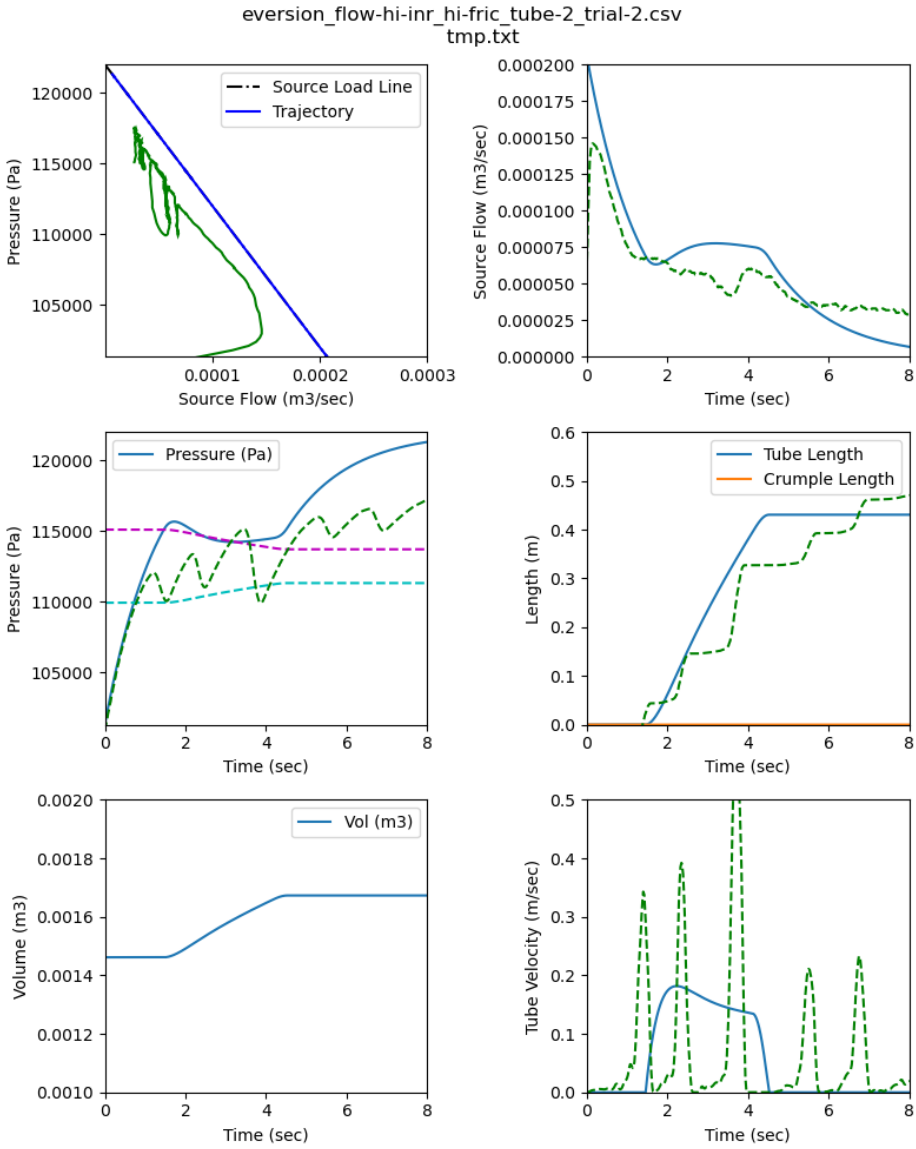


Figure 3: Comparison of one experimental run (green dashed line) with a simulation (solid blue line) using an initial set of parameter values (Table 2).

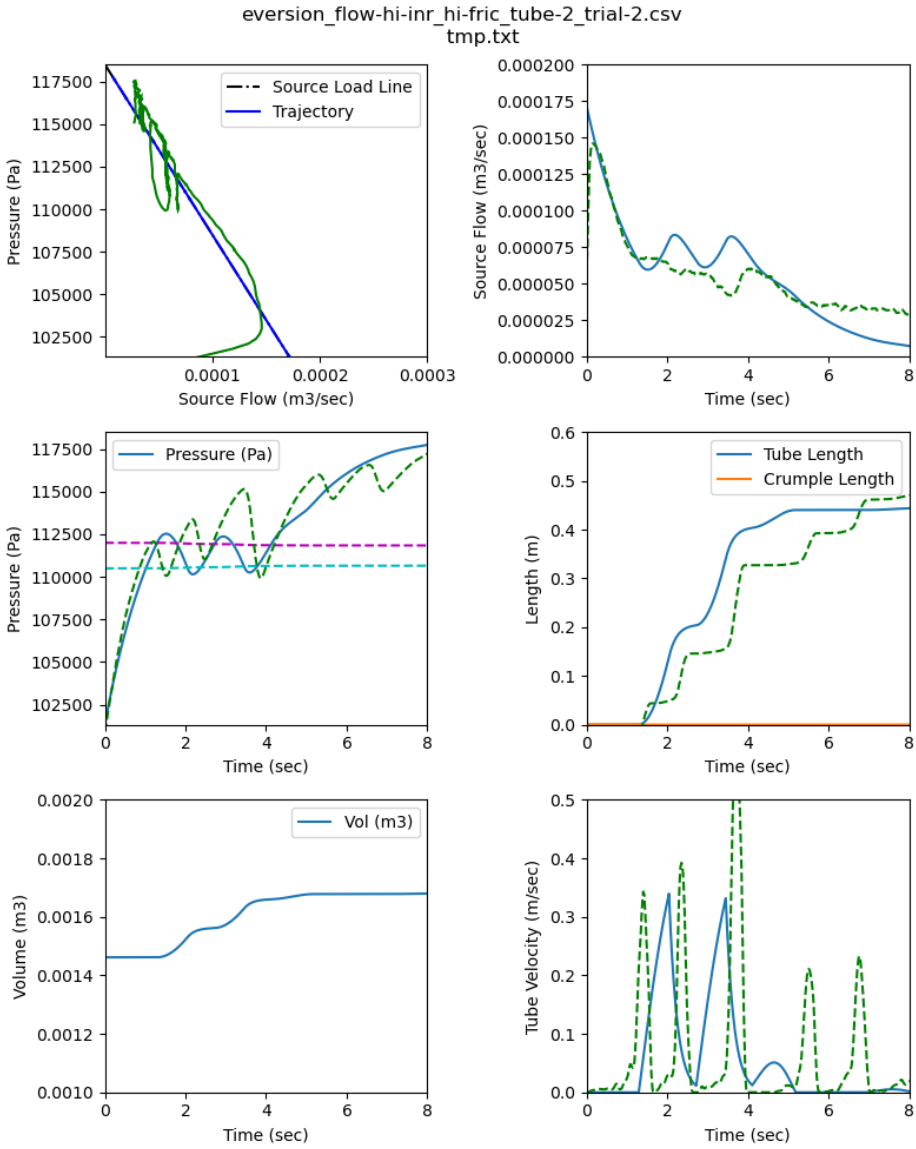


Figure 4: The same simulation and data (See Lewis, Fig 9, hiI, hiTf) with manually tuned parameter values (Table 4

| Parameter | Value | Units |
|---|---|---|
| ET_RofL_mode | constant | text |
| ET_radius | 1.2500E-02 | m |
| J | 5.6400E-04 | kg/m2 |
| K2drag | 1.0000E+01 | Nm |
| Kdrag | 8.0000E+00 | N/m2/sec |
| LLine_SIu | 1.0000E-08 | m3/sec/Pascal |
| Lmax | 6.0000E-01 | m |
| PBA_static | 1.1511E+05 | Pascals |
| PHalt_dyn | 1.0994E+05 | Pascals |
| Patmosphere | 1.0132E+05 | Pascals |
| Psource_SIu | 1.2201E+05 | Pascals |
| RT | 2.4560E+03 | ?? |
| Rsource_SIu | 1.0000E+08 | Pa/m3/sec |
| T | 2.9540E+02 | K |
| Tau_coulomb | 6.9400E-02 | Nm |
| Threshold Taper | 3.2319E+03 | Pa/m |
| Vhousing_m3 | 1.4616E-03 | m3 |
| dt | 2.5000E-03 | sec |
| et_MPM | 1.0000E-01 | kg/m |
| rReel | 1.0900E-02 | m |

Table 2: Initial parameter values for the simulation before parameter tuning (Figure 3

| Parameter | Value | Units |
|---|---|---|
| ET_RofL_mode | constant | text |
| ET_radius | 1.2500E-02 | m |
| J | 5.6400E-04 | kg/m2 |
| K2drag* | 5.0000E-01 | Nm |
| Kdrag* | 1.0000E+00 | N/m2/sec |
| LLine_SIu | 1.0000E-08 | m3/sec/Pascal |
| Lmax* | 6.5000E-01 | m |
| PBA_static* | 1.1200E+05 | Pascals |
| PHalt_dyn* | 1.1050E+05 | Pascals |
| Patmosphere | 1.0132E+05 | Pascals |
| Psource_SIu* | 1.1850E+05 | Pascals |
| RT | 2.4560E+03 | ?? |
| Rsource_SIu | 1.0000E+08 | Pa/m3/sec |
| T | 2.9540E+02 | K |
| Tau_coulomb | 6.9400E-02 | Nm |
| Threshold Taper* | 3.5000E+02 | Pa/m |
| Vhousing_m3 | 1.4616E-03 | m3 |
| dF1dL | 3.6364E+00 | N/m?? |
| dt | 2.5000E-03 | sec |
| et_MPM | 1.0000E-01 | kg/m |
| rReel | 1.0900E-02 | m |

Table 3: Final parameter values after parameter tuning on the same data set (Figure 4). '*' indicates parameter was modified to improve fit.

Table 4: Parameter values for the two-compartment model fit (Figure **??**).

# 4 Model Refinements

## 4.1 Multiple compartment model

The results of the one-compartment model illustrate a limitation that its pressure-flow behavior is limited to a straight line. We noted loops in the pressure-flow plane (Figure 4, upper-left) in which a growing ET deviated significantly from the source load line. This indicates that air pressure does not instantaneously equilibrate along the ET, but instead takes time to flow from the tubing compartment down to new volume at the growing tip. A lumped parameter model of this flow can be formed of two compartments: one compartment is the reel housing from which the tube is everted, and the second compartment is the tubing. A flow resistance, $R_T(L)$, connects the two chambers and this resistance increases with length. Initially we assume that the flow resistance between compartments is a fixed ratio (ET_Res_ratio) of the source resistance (Rsource_SIu). Length dependence of the resistance will be introduced later if needed. The tubing volume increases with length (as it did in Eqn 1). Such a model is shown in Figure **??** (Right).

Two add the second compartment, representing the everting tube volume and associated flow, we need to expand our model state variables as follows:

$$\begin{aligned} N, \dot{N} &\rightarrow \{N_1, N_2, \dot{N}_1, \dot{N}_2\} \\ V_t &\rightarrow \{V_{housing}, V_T(L)\} \\ f_{source} &\rightarrow \{f_{source}, f_{int}, f_T\} \\ P &\rightarrow \{P_{C1}, P_{C2}\} \end{aligned} \tag{24}$$

where $N_1$ and $N_2$ are the molar quantity of air in the housing and tube respectively, $f_i$ are the respective flows indicated in Figure **??** (Right), and $P_{C1}$ and $P_{C2}$ are the pressures in the housing and tube respectively.

We then have new equations to replace or expand Equations 5, 14, and 15 as follows:

$$\dot{N}_1 = (f_{source} - f_{int} - f_T) \cdot \text{moles\_per\_m3} \tag{25}$$

$$\dot{N}_2 = f_T \cdot \text{moles\_per\_m3} \tag{26}$$

$$P_{C1} = \frac{N_1 RT}{V_{housing}} \tag{27}$$

$$P_{C2} = \frac{N_2 RT}{V_T(L)} \tag{28}$$

$$f_{source} = (P_{source} - P_{C1})/R_{source} \tag{29}$$

$$f_T = (P_{C1} - P_{C2})/R_T(L) \tag{30}$$

$$f_{int} = f_{source} - f_T \tag{31}$$

# 5 Results of Two Compartment Model

The same data set as in Figure 4 were simulated with the two-compartment version of the model (Figure 5). Flow resistance between reel housing (compartment 1) and the ET was approximated by a ratio of Rsource_SIu. Parameter set is given in Table **??**.

Results from Tube 1, Trial 2 (hi inertia, hi friction) are given in Figure 5. Notably, the simulated tube pressure deviates below the source loadline during the start-stop oscillations similar to the experimental data.

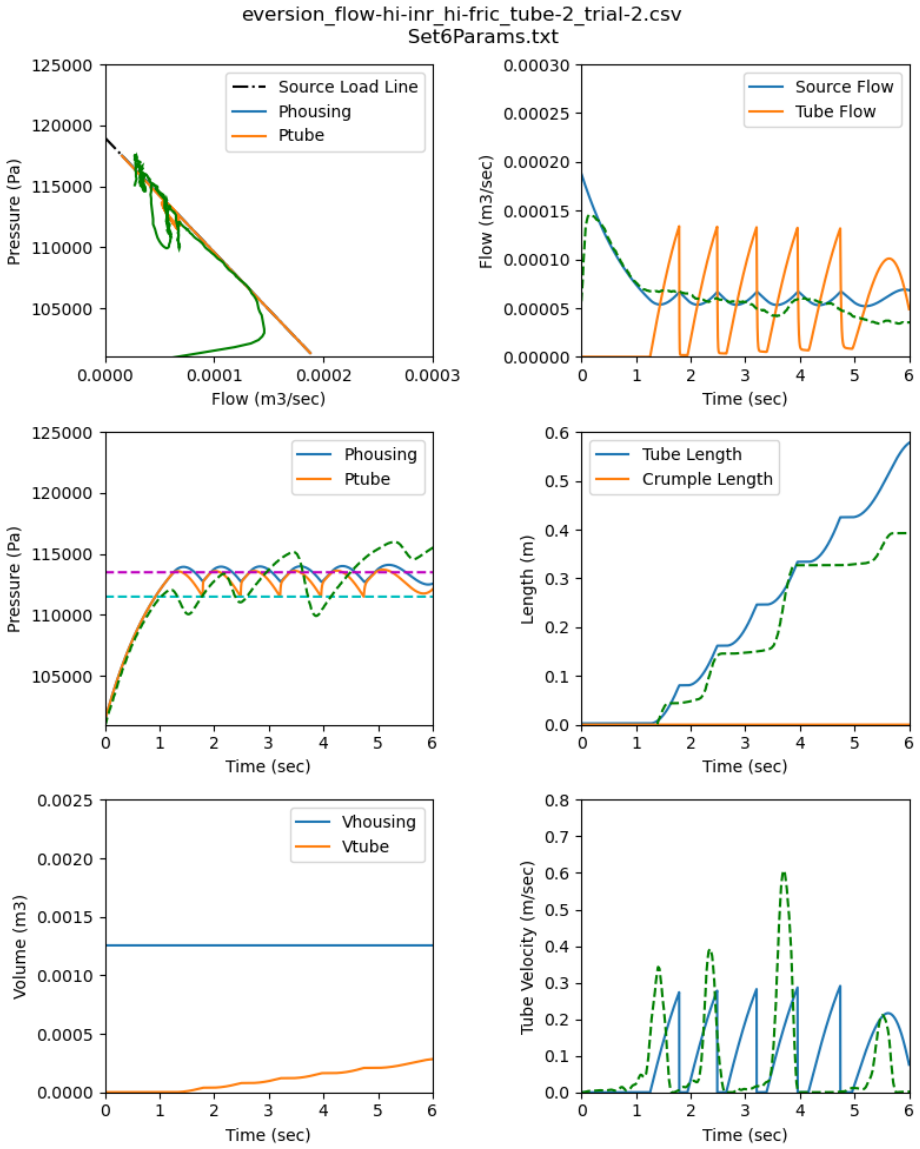


Figure 5: Two compartment model compared with same data as Figure **??**. Two compartment model allows simulation to deviate from the diagonal load line (orange trace, Upper Left).

## 5.1 Additional Two-Compartment Fits

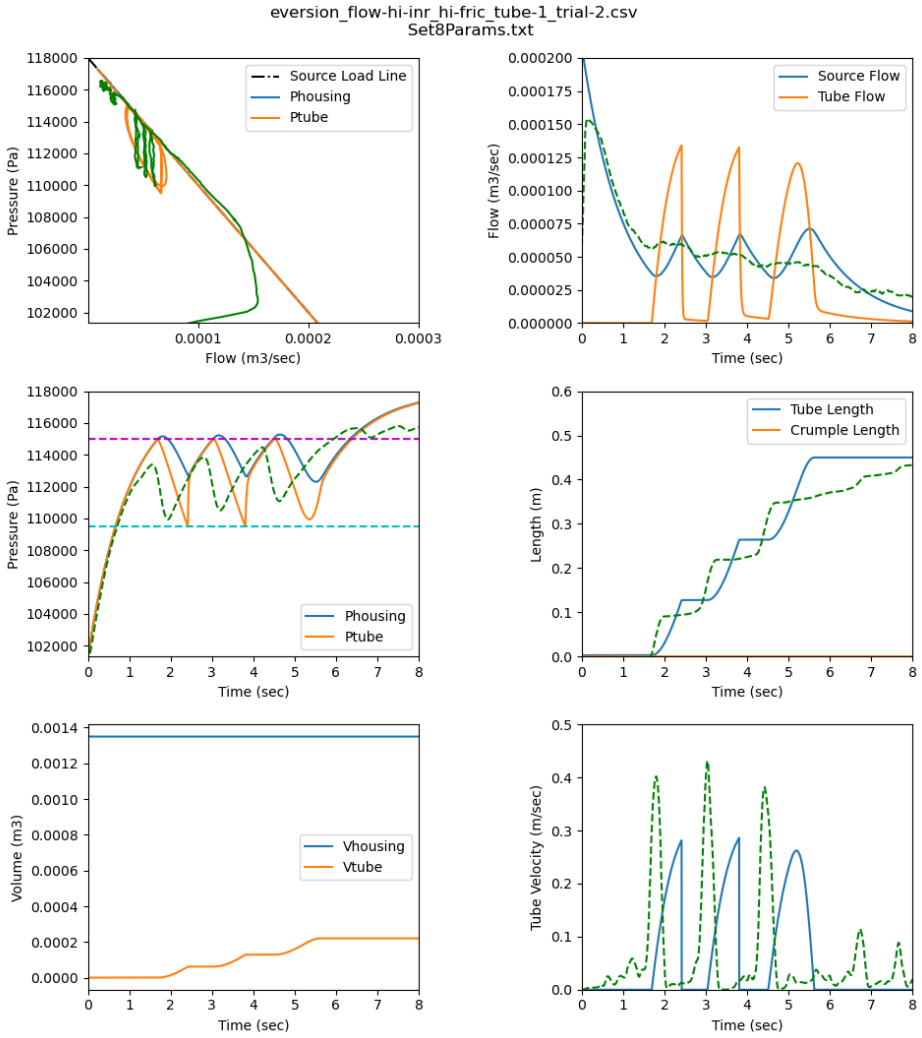


Figure 6: Two compartment model compared with simulation (See Lewis, Fig 9, hiI, hiTf)

## 5.2 Varying tube profile

While most ET research uses tubing of constant diameter, the effective diameter of an ET can vary with length in two main ways. First, the tube can be fabricated with variable diameter by thermal welding of two sheets. Second, tubing of constant diameter may be everted into a tubular space of changing diameters. While the mechanics of eversion will in general be different in these two cases, we will initially ignore that difference and make tube diameter a function of eversion distance $L$, $V(L)$.

Tube profiles

Simulations

# References

[1] Laura H Blumenschein, Allison M Okamura, and Elliot W Hawkes. Modeling of bioinspired apical extension in a soft robot. In *Conference on Biomimetic and Biohybrid Systems*, pages 522–531. Springer, 2017.

[2] Panagiotis Vartholomeos, Zicong Wu, Hadi Sadati, and Christos Bergeles. Lumped parameter dynamic model of an eversion growing robot: Analysis, simulation and experimental validation. In *IEEE International Conference on Robotics and Automation (ICRA)*, 2024.